

AMITE: A Novel Polynomial Expansion for Analyzing Neural Network Nonlinearities

Mauro J. Sanchirico III, Xun Jiao, and C. Nataraj

Abstract—Polynomial expansions are an important technique in the analysis and study of neural network nonlinearities. Recently, expansions have been applied to neural networks addressing well known difficulties in the verifiable, explainable and secure deployment thereof. Existing approaches span classical Taylor and Chebyshev methods, asymptotics, and many numerical and algorithmic approaches. We find that while existing approaches individually have useful properties such as exact error formulas, monic form, adjustable domain, and robustness to undefined derivatives, there are no approaches that provide a consistent method yielding an expansion with all these properties. To address this gap, we develop an analytically modified integral transform expansion referred to as AMITE, which is a novel expansion via integral transforms modified using derived criteria for convergence. We apply AMITE to the nonlinear activation functions of neural networks including hyperbolic tangent and rectified linear units. Compared with existing state-of-the-art expansion techniques such as Chebyshev, Taylor series, and numerical approximations, AMITE is the first polynomial expansion that can provide six previously mutually exclusive desired expansion properties such as exact formulas for the coefficients and exact expansion errors (Table II). Using an MLP as a case study, we demonstrate the effectiveness of AMITE in the equivalence testing problem of MLP where a black-box network under test is stimulated, and a replicated multivariate polynomial form is efficiently extracted from a noisy response to enable comparison against an original network. AMITE presents a new dimension of expansion methods that are suitable for analysis/approximation of nonlinearities in neural networks, which opens up new directions and opportunities for the theoretical analysis and systematic testing of neural networks.

Index Terms—Neural Networks, Equivalence, Taylor, Fourier, Polynomial, Approximation.

I. INTRODUCTION

IN the design and implementation of nonlinear systems, polynomial expansions provide an important means of decomposing nonlinear functions into a form facilitating analysis. The emerging neural networks have inherent nonlinearities in their activation functions such as hyperbolic tangent and rectified linear units. Various polynomial expansions and approximations have been applied to nonlinear activations of neural networks to enable explainable, verifiable, and secure deployment of neural systems, with [1], [2], and [3] being three recent examples respectively. The motivation to develop explainability and verification techniques is further enhanced

TABLE I
QUALITATIVE PROPERTIES CONSIDERED FOR A POLYNOMIAL EXPANSION
OF THE FORM: $\varphi(v) = \sum_m \alpha_m^M v^m + H_M(v)$

Property	Description
<i>Exact Coeffs.</i>	Precise analytic equations available for the coefficients, α_m , for the nonlinearities considered.
<i>Explicit Exact Errors</i>	Precise analytic equations are explicitly worked for the expansion errors, $H_M(v)$.
<i>Monic Form</i>	The expansion is formulated directly as a sum of monomials, i.e. $\sum_m \alpha_m v^m$ and not as a sum of other polynomials or piecewise polynomials.
<i>Adjustable Domain</i>	The approximation $\varphi(v) = \sum_m \alpha_m v^m$ is valid for any desired domain of validity $ v < V$ without transforming or re-scaling v .
<i>Handles undef. derivs.</i>	The expansion is valid if some of the derivatives of φ are undefined.
<i>Consistent Method</i>	The method can be applied consistently to a wide variety of functions without ad-hoc modifications.

by proposed use of neural networks in critical fielded systems such as unmanned aerial vehicles [4], [5] and hypersonic vehicles [6]. Meanwhile, use of neural networks in healthcare applications, such as [7], further drives the need to develop secure inference techniques to protect third party private information [3], [8]. The polynomial expansion of neural network activation functions is a method employed in addressing all of these diverse and important challenges.

Existing polynomial expansions of neural nonlinearity can be categorized as follows. First, the well-known Taylor series is employed often in the study of neural nonlinearities [1], [19]–[23]. While Taylor series provides the advantage of exact formulas for coefficients and errors and often provides a useful local approximation, its domain of validity is limited to $|v| < \frac{\pi}{2}$ for $\tanh(v)$ nonlinearities [18] and it requires that a function have defined derivatives in the domain where the expansion must be valid. A well known identity which is valid for large arguments is given: $\tanh(v) = 1 + 2 \sum_{m=1}^{\infty} (-1)^m e^{-2mv} \forall v > 0$ [24], and can be manipulated into a power series like form by expanding e^{-2mv} . However, the result is still not valid for small v . Similarly, a number of asymptotic series are often available for nonlinear functions such as \tanh but are often only valid in certain domains (e.g. large arguments) [9], do not have a monic form, and as such are not generally differentiable [24].

A Chebyshev approximation can be applied using recursive formulas for the coefficients [11]. References employing Chebyshev approximations or comparing them to other

M. Sanchirico is with the Lockheed Martin Corporate Technology Office, Shelton CT, 06484 USA and the Department of Electrical and Computer Engineering, Villanova University, Villanova PA, 19085 USA

X. Jiao is with the Department of Electrical and Computer Engineering, Villanova University, Villanova, PA, 19085 USA

C. Nataraj is with the Villanova Center for Analytics of Dynamic Systems (VCADS), Villanova University, Villanova, PA, 19085 USA

TABLE II
QUALITATIVE COMPARISON OF POLYNOMIAL EXPANSION TECHNIQUES AVAILABLE FOR NEURAL NETWORK NONLINEARITIES

	<i>Exact Coeffs.</i>	<i>Explicit Exact Errors</i>	<i>Monic Form</i>	<i>Adjustable Domain</i>	<i>Handles Undef. Derivs.</i>	<i>Consistent Method</i>
AMITE	Y	Y	Y	Y	Y	Y
Asymptotics [9]	Y				Y	
Bernstein [10]	Y			Y	Y	Y
Chebyshev [11]	Y				Y	Y
Exponential Chebyshev [12]	Y			Y	Y	Y
Fast Fourier-Legendre [13]					Y	Y
Least Squares Regression [3]			Y	Y	Y	Y
Minimax w. Chebyshev [3], [14]				Y	Y	Y
Piecewise [15]				Y	Y	
Recursive Regression [2]				Y	Y	Y
Remez / Modified Remez [16], [17]				Y	Y	Y
Taylor [18]	Y	Y	Y			Y

approximations for neural nonlinearities include [14], [25] and [3]. Alternatively, the Fourier-Legendre series [26] has well-known methods for fast coefficient computation [13] and provides a fast rate of convergence. The Bernstein basis is employed by Huang et al. in ReachNN to perform reachability analysis for neural controlled systems [10]. Overall, the related polynomial basis techniques via Chebyshev, Fourier-Legendre, Bernstein and similar methods provide accurate approximation with the useful property that formulas for coefficients can be exact using some methods. However, while most methods employing such techniques provide upper bounds on the error, exact error formulas have not yet been provided for the expansions of the neural nonlinearities considered.

If analytic formulas are not required, many numerical techniques are available to approximate a nonlinearity. Obla et al. compare least squares and best uniform approximation (i.e. minimax approximation) against Taylor series [3]. Lee et al. also use a minimax approximation with a Chebyshev basis [14], improving upon results from a modified Remez algorithm [16]. Numerically fit piecewise polynomials are suited for efficient implementation of a nonlinear function such as tanh over a wide domain [27], [28]. Piecewise approximations can be combined with other methods, e.g. Chebyshev [15].

Piecewise linear polynomials specifically are well suited to relu nonlinearities which are a special case thereof. They are key components of the Marabou framework for verification of deep neural networks [29] and employed by Dutta et al. to perform reachability analysis via regressive polynomial rule inference [2]. Dutta et al. further reduce the expansion error by repeatedly fitting a low order polynomial and fitting a new polynomial to the residual. This recursive approach keeps the resulting polynomial order low but does not lend itself to extraction of exact error formulas, which the authors cite as a challenge and then solve by further reducing the polynomial to a piecewise linear model [2].

To address the limitations of many existing polynomial approximations, we employ a special functions approach to develop a new polynomial expansion technique, applicable to a wide class of neural network nonlinearities and having as many

of the desirable properties of the above expansions including many that were previously mutually exclusive. Motivated by applications to verification and security noted above, we provide, for the first time, the derivation of explicit exact error formulas and useful analytic approximations thereof. To facilitate mathematical manipulation, we provide a monic polynomial form like that of the Taylor series and an adjustable domain of convergence that does not require transformation or re-scaling. We provide exact coefficients that do not require iteration or recursion to compute and avoid the main disadvantage of the Taylor series by remaining robust to undefined derivatives. Furthermore, the method provides a consistent approach which can be readily applied to a wide variety of nonlinear functions without *ad hoc* manipulation for a specific nonlinearity type.

The expansion is developed using integral transforms of the generalized Fourier type, modified according to derived criteria for convergence and as such is called the analytically modified integral transform expansion (AMITE) technique. The qualitative expansion properties that we consider are defined in Table I. We present a comprehensive comparison of AMITE with existing state-of-the-art expansion methods with respect to these properties in Table II.

We summarize our contribution as follows.

- We develop a novel polynomial expansion technique, the analytically modified integral transform expansion (AMITE), via a special functions approach to enable decomposing neural network activation functions into polynomial forms having several advantageous properties, listed in Table II, many of which are otherwise mutually exclusive. The expansion is carried out explicitly for the hyperbolic tangent and ReLU nonlinearities and exact error formulas are derived and analyzed via exploitation of a number of non-trivial relationships amongst the special and elementary functions.
- Using a single hidden layer MLP as a case study, we demonstrate use of the AMITE technique in a black-box system identification based equivalency test for checking that a given MLP is output-equivalent to another. While

similar methods would require piecewise polynomials or numerical fits due to the limitations of existing expansions available for neural nonlinearities, we show that we can efficiently expand the entire MLP as a single multivariate polynomial approximation. This is enabled by the adjustable domain of convergence and simple monic form, and is advantageous for facilitating exact error analysis. This improvement combined with the newly developed exact formulas implies that the AMITE technique is a useful complement to the existing panoply of polynomial expansions employed in the analysis of neural systems.

Organization of the paper: Section II defines the notation and assumptions. The main expansion formulas and errors are developed in Section III and expansion results are summarized in Section IV. The case study for application to single hidden layer MLP is presented in Section V. Related work is reviewed in Section VI and Section VII concludes the paper.

II. DEFINITIONS AND PROBLEM FORMULATION

The nonlinearities considered in this paper are of the hyperbolic tangent type, i.e.

$$\tanh(v) = \frac{e^v - e^{-v}}{e^v + e^{-v}}, \quad \text{relu}(v) = \frac{|v| + v}{2}. \quad (1)$$

When developing approximations of activation functions φ we denote the approximation coefficients α_m such that

$$\varphi(v) \simeq \sum_{m=0}^M \alpha_m v^m \quad (2)$$

We consider MLPs having N_I inputs and N_H hidden neurons. Input layer weights and biases are denoted $W^{\{0\}} = [w_{n,i}^{\{0\}}] \in \mathcal{M}^{N_H \times N_I}$ and $b^{\{0\}} = [b_n] \in \mathcal{M}^{N_H \times 1}$. Hidden layer weights and bias are denoted $w^{\{1\}} = [w_n^{\{1\}}] \in \mathcal{M}^{1 \times N_H}$ and $b^{\{1\}} \in \mathcal{M}^{1 \times 1}$. The network has the activation function $\varphi(v)$. The weights and biases for a given network are collectively denoted $\beta = \{W^{\{0\}}, w^{\{1\}}, b^{\{0\}}, b^{\{1\}}\}$. Such a network has the input-output relationship:

$$y(\alpha, \beta, x) = w^{\{1\}} \varphi(W^{\{0\}}x + b^{\{0\}}) + b^{\{1\}} \quad (3)$$

The input to hidden neuron n is denoted

$$v_n = b_n^{\{0\}} + \sum_{i=1}^{N_I} w_{n,i}^{\{0\}} x_i \quad \forall \quad n \in [1, N_H]. \quad (4)$$

We define an *original network* to be a neural network, or a sub-circuit thereof, that is created by a designer, e.g. in software. Similarly, we define the *network under test* to be the implemented neural network (e.g. in hardware), or a sub-circuit thereof, which a test procedure must determine to be output-equivalent to the original network. The *stimulus signal* is the signal applied and the *response signal* is the output signal measured, including measurement noise. The *replicated network* is defined as the network having weights extracted from the network under test. A network under test is confirmed to be *output-equivalent* to the original network if it is shown

that they will produce sufficiently close outputs for all inputs in a given interval, according to a provided error metric.

Assumptions: We make the following assumptions in developing the expansion and demonstrating its example application.

1) *Form of the nonlinear activations:* We assume that nonlinearities, φ , to be analyzed can be represented by integral transforms in the form of $\varphi(v) = \int_{\mathbb{R}} \Phi(\xi) f(\xi v) d\xi$ wherein the kernels have Taylor series convergent on $(-\infty, \infty)$ of the form $f(\xi v) = \sum_{m=0}^{\infty} f(m)(\xi v)^m$.

2) *Low-dimensional inputs:* For the example equivalence test, formulas are provided for n -dimensional inputs; however, the test is only practical for networks having a small number of inputs, such as those that may be used in neural control applications.

3) *Normalized inputs:* For the example equivalence test, we assume that at test time knowledge of the largest possible magnitudes of all network inputs is available. Without loss of generality, we use inputs x_i normalized such that $x_i \in [-1, 1]$.

4) *Assumed Structure:* For the example equivalence test, the *expected structure* (i.e. expected number of inputs and hidden nodes) of the network under test is assumed to be known. The *actual structure* of the network under test is assumed to be unknown.

III. AMITE DEVELOPMENT

To achieve the expansion properties shown in Table II for the AMITE technique we seek expressions of the forms:

$$\tanh(v) \simeq \sum_{m=0}^M T_{2m+1}(M) v^{2m+1}, \quad \forall \quad |v| < V, \quad (5)$$

$$\text{relu}(v) \simeq \frac{v}{2} + \sum_{m=0}^M R_{2m}(M) v^{2m}, \quad \forall \quad |v| < V. \quad (6)$$

In (5) and (6) we require explicit formulas suitable for evaluation in arbitrary precision, yielding expansions valid out to a tunable desired bound of validity V which can be made arbitrarily large. The coefficients are allowed to depend on the order of expansion M . We present an exposition of the general expansion method which can be applied to a wide class of activations. We then begin application of the method to our specific activations with an alternate derivation of the Taylor series of $\tanh(v)$ formulated to illuminate the source of divergence in the unmodified expansion, making apparent how it can be modified to achieve our desired properties in Table II. We then apply the method explicitly to $\tanh(v)$, $\text{relu}(v)$, and finally to a single hidden layer MLP as a whole.

A. General Expansion Technique

Our general method for obtaining the coefficients is as follows. First, the function φ to be approximated is expressed via an integral transform of the form:

$$\varphi(v) = \int_{\mathbb{R}} \Phi(\xi) f(\xi v) d\xi. \quad (7)$$

We find the Fourier transform family well suited to this step. The kernel $f(\xi v)$ is then expanded via the truncated Taylor series

$$f(\xi v) \simeq \sum_{m=0}^M \tilde{f}(m)(\xi v)^m + \Upsilon_M^{\{f\}}(\xi v), \quad (8)$$

$$\varphi(v) \simeq \int_{\mathbb{R}} \Phi(\xi) \sum_{m=0}^M \tilde{f}(m)(\xi v)^m d\xi. \quad (9)$$

The remainder $\Upsilon_M^{\{f\}}(\xi v)$ is factored into parts $P_M(\xi v)$ and $Q_M(\xi v)$ that increase with and without bound respectively

$$\Upsilon_M^{\{f\}}(\xi v) = P_M(\xi v)Q_M(\xi v). \quad (10)$$

The dominating term $Q_M(\xi v)$ is set equal to a constant C and solved for ξ to determine a suitable limit $\xi = \rho(M)$ of integration for (9) which remains in the region of convergence of (8), i.e. $\xi = Q_M^{-1}(C)/v$. In cases where v can take on one of many values, the limit of integration can be defined with respect to its maximum value V to err on the side of safety.

$$\rho_V(M) = Q_M^{-1}(C)/V \quad (11)$$

The integral of (9) can then be rewritten as

$$\varphi(v) \simeq \sum_{m=0}^M \tilde{f}(m)v^m \int_{-\rho_V(M)}^{\rho_V(M)} \Phi(\xi)\xi^m d\xi. \quad (12)$$

where the exchange of the summation and the integral is permitted since the integral is bounded to the convergent region $(-\rho_V(M), \rho_V(M))$. Solving the remaining integral yields an approximation in the desired form of (2).

By noting the parts of (9) left out by the adjustments an exact expression for the remainder $H_M^{\{\varphi\}}(v)$ is revealed

$$\begin{aligned} H_M^{\{\varphi\}}(v) &= \int_{-\rho_V(M)}^{\rho_V(M)} \Phi(\xi)\Upsilon_M^{\{f\}}d\xi \\ &+ \int_{-\infty}^{-\rho_V(M)} \Phi(\xi)f(\xi v)d\xi + \int_{\rho_V(M)}^{\infty} \Phi(\xi)f(\xi v)d\xi \end{aligned} \quad (13)$$

such that the expansion and its coefficients are given as

$$\varphi(v) = \sum_{m=0}^M \alpha_m(M)v^m + H_M^{\{\varphi\}}(v) \quad (14)$$

$$\simeq \sum_{m=0}^M \alpha_m(M)v^m \quad \forall |v| < V$$

$$\alpha_m(M) = \tilde{f}(m) \int_{-\rho_V(M)}^{\rho_V(M)} \Phi(\xi)\xi^m d\xi \quad (15)$$

B. Alternate Taylor Series Derivation

We derive the Taylor series of $\tanh(v)$ by expressing it in terms of its Fourier transform. Identities from [30] yield

$$\tanh(v) = \lim_{\rho \rightarrow \infty} \int_0^\rho \operatorname{csch}\left(\frac{\pi}{2}\xi\right) \sin(\xi v) d\xi. \quad (16)$$

Expanding the kernel $\sin(\xi v)$ to a partial sum yields

$$\begin{aligned} \tanh(v) &\simeq \\ \lim_{\rho \rightarrow \infty} \sum_{m=1}^M \frac{(-1)^{m-1}v^{2m-1}}{(2m-1)!} \int_0^\rho \xi^{2m-1} \operatorname{csch}\left(\frac{\pi}{2}\xi\right) d\xi. \end{aligned} \quad (17)$$

Noting the identity

$$\int_0^\infty \xi^{2m-1} \operatorname{csch}(a\xi) d\xi = \frac{2^{2m}-1}{2m} \left(\frac{\pi}{a}\right)^{2m} |B_{2m}|, \quad (18)$$

from [24] and applying to (17) yields the familiar Taylor series

$$\tanh(v) \simeq \sum_{m=1}^M \frac{2^{2m}(2^{2m}-1)B_{2m}v^{2m-1}}{(2m)!}, \quad \forall |v| < \frac{\pi}{2}. \quad (19)$$

Noting that the manipulations of (17) are only valid within the convergent regions of the Taylor expansions of the kernel $\sin(\xi v)$ illuminates the source of the divergence for $|v| \geq \pi/2$. We illustrate in the following section how this can be mitigated while preserving accuracy over an arbitrary interval.

C. Modifying the Limits of Integration

To modify the integral of Eq. (17) so that the resulting expansions are valid for $|v| \geq \frac{\pi}{2}$ we require a suitable upper bound ρ accounting for the domain of validity of the M -term partial sum expansions of the kernel. Following section III-A we begin by factoring the remainders of the partial sums to consider the dominant factors which contribute to their divergence. We treat both $\sin(\xi v)$ and $\cos(\xi v)$ which we will employ in the next sections to expand $\tanh(v)$ and $\operatorname{relu}(v)$ respectively. We begin with the partial sum formulas

$$\cos(u) = \sum_{m=0}^M \frac{(-1)^m u^{2m}}{(2m)!} + \Upsilon_M^{\{\cos\}}(u), \quad (20)$$

$$\sin(u) = \sum_{m=0}^M \frac{(-1)^m u^{2m+1}}{(2m+1)!} + \Upsilon_M^{\{\sin\}}(u), \quad (21)$$

having remainders given by

$$\Upsilon_M^{\{\cos\}}(u) = (-1)^{M+1} u^{2M+2} \sum_{m=0}^{\infty} \frac{(-1)^m u^{2m}}{(2m+2M+2)!}, \quad (22)$$

$$\Upsilon_M^{\{\sin\}}(u) = (-1)^{M+1} u^{2M+3} \sum_{m=0}^{\infty} \frac{(-1)^m u^{2m}}{(2m+2M+3)!}. \quad (23)$$

Factoring the remainders in the form of (10) yields

$$\begin{aligned} \Upsilon_M^{\{\cos\}}(u) &= \\ \frac{(-1)^{M+1} u^{2M+2}}{(2M+2)!} {}_1F_2\left(1; M+2, M+\frac{3}{2}; -\frac{u^2}{4}\right), \end{aligned} \quad (24)$$

$$\begin{aligned} \Upsilon_M^{\{\sin\}}(u) &= \\ \frac{(-1)^{M+1} u^{2M+3}}{(2M+3)!} {}_1F_2\left(1; M+2, M+\frac{5}{2}; -\frac{u^2}{4}\right). \end{aligned} \quad (25)$$

As u tends to infinity the hypergeometric factors in (24) and (25) tend to zero and the outer factors

$$Q_M^{\{\cos\}}(u) = \frac{u^{2M+2}}{(2M+2)!}, \quad Q_M^{\{\sin\}}(u) = \frac{u^{2M+3}}{(2M+3)!}, \quad (26)$$

tend to infinity. Noting that the outer factors drive the remainders' growth we define the range of validity of the partial sums in (20) and (21) to be all u such that $Q_M^{\{\cos\}}(u) < 1$ and

$Q_M^{\{\sin\}}(u) < 1$ respectively. Thus yielding the required bounds on the domain of validity of each partial sum:

$$\cos(u) \simeq \sum_{m=0}^M \frac{(-1)^m u^{2m}}{(2m)!} \quad \forall u < ((2M+2)!)^{\frac{1}{2M+2}}, \quad (27)$$

$$\sin(u) \simeq \sum_{m=0}^M \frac{(-1)^m u^{2m+1}}{(2m+1)!} \quad \forall u < ((2M+3)!)^{\frac{1}{2M+3}}. \quad (28)$$

Noting the argument to the kernel in (17) is $u = \xi v$, and adjusting for the maximum value $V = \max(v)$, we let σ and τ denote the required upper bounds for integrals in the forms $\int \Phi(\xi) \cos(\xi v) d\xi$ and $\int \Phi(\xi) \sin(\xi v) d\xi$ respectively:

$$\sigma = \frac{((2M+2)!)^{\frac{1}{2M+2}}}{V}, \quad \tau = \frac{((2M+3)!)^{\frac{1}{2M+3}}}{V}. \quad (29)$$

D. An Improved Hyperbolic Tangent Expansion

Having identified the appropriate bound, τ , for integrals having kernels $\sin(\xi v)$ we can now return to (17) and integrate the component $\Lambda_j(\xi) = \int \xi^j \operatorname{csch}\left(\frac{\pi}{2}\xi\right) d\xi$ from 0 to τ to yield the desired formulas for the coefficients $T_{2m+1}(M)$ in eq. (5).

$$\begin{aligned} \tanh(v) &= \sum_{m=0}^M T_{2m+1}(M) v^{2m+1} + H_M^{\{\tanh\}}(v) \\ &\simeq \sum_{m=0}^M T_{2m+1}(M) v^{2m+1} \quad \forall |v| < V, \end{aligned} \quad (30)$$

$$\begin{aligned} T_{2m+1}(M) &= \frac{2^{2m+1}(4^{m+1} - 1)B_{2m+2}}{(m+1)(2m+1)!} \\ &+ \frac{(-1)^{m+1}4}{\pi} \sum_{k=0}^{2m+1} \frac{2^k \tau^{2m+1-k} \chi_{k+1} \left(e^{-\frac{\pi\tau}{2}}\right)}{\pi^k (2m+1-k)!}. \end{aligned} \quad (31)$$

Here, $\chi_s(z) = \frac{1}{2}(\operatorname{Li}_s(z) - \operatorname{Li}_s(-z))$ denotes Legendre's Chi function. The result of (31) is derived fully in Appendix A. The precise remainder follows directly from application of (13):

$$\begin{aligned} H_M^{\{\tanh\}}(v) &= \int_{\tau}^{\infty} \operatorname{csch}\left(\frac{\pi}{2}\xi\right) \sin(\xi v) d\xi \\ &+ \frac{(-1)^{M+1}v^L}{L!} \int_0^{\tau} \xi^L \operatorname{csch}\left(\frac{\pi}{2}\xi\right) {}_1F_2(1; b_1, b_2; z) d\xi, \end{aligned} \quad (32)$$

$$L = 2M + 3, b_1 = M + 2, b_2 = M + \frac{5}{2}, z = -\frac{v^2 \xi^2}{4}. \quad (34)$$

The second term (33) dominates for large v due to the v^L factor, causing the expected divergence for $|v| \geq V$. Since (33) follows directly from the Taylor remainder $\Upsilon_M^{\{\sin\}}(\xi v)$ it is by definition small for v within the region of convergence. Meanwhile, the first term (32) dominates for small v leading to Gibbs-like oscillation of the error for $|v| < V$. Noting this effect, the integral of (32) can be solved exactly to analyze the error inside the region of convergence for an M term expansion. Let $I_M^{\{\tanh\}}(v)$ denote this error component:

$$I_M^{\{\tanh\}}(v) = \int_{\tau}^{\infty} \operatorname{csch}\left(\frac{\pi}{2}\xi\right) \sin(\xi v) d\xi \quad (35)$$

$$\begin{aligned} &= 2 \tanh(v) - \frac{i}{\pi} (B_{e^{\pi\tau}}(a, 0) - B_{e^{\pi\tau}}(a^*, 0)), \\ &a = \frac{1}{2} + \frac{iv}{\pi}. \end{aligned} \quad (36)$$

Here, $B_z(a, b)$ denotes the Incomplete Beta function. We first rearrange (35) to extract the dominant oscillating factor. Noting that $B_{e^{\pi\tau}}\left(\frac{1}{2} \pm \frac{iv}{\pi}, 0\right)$ can be factored as

$$\begin{aligned} B_{e^{\pi\tau}}\left(\frac{1}{2} \pm \frac{iv}{\pi}, 0\right) &= \\ &\frac{e^{\frac{\pi\tau}{2}} e^{\pm i\tau v}}{\frac{1}{2} \pm \frac{iv}{\pi}} {}_2F_1\left(1, \frac{1}{2} \pm \frac{iv}{\pi}; \frac{3}{2} \pm \frac{iv}{\pi}; e^{\pi\tau}\right) \end{aligned} \quad (37)$$

and substituting this result (37) into (35) reveals

$$\begin{aligned} I_M^{\{\tanh\}}(v) &= \frac{e^{\frac{\pi\tau}{2}}}{e^{\pi\tau} - 1} (UF + U^*F^*), \\ U &= \frac{e^{-i\tau\pi}}{v - \frac{i\pi}{2}}, \quad F = {}_2F_1\left(1, 1; \frac{3}{2} + \frac{iv}{\pi}; \frac{1}{1 - e^{\pi\tau}}\right). \end{aligned} \quad (39)$$

Recalling from (29) that τ increases with respect to the number of terms M and noting that

$$\lim_{\tau \rightarrow \infty} {}_2F_1\left(1, 1; c; \frac{1}{1 - e^{\pi\tau}}\right) = 1 \quad (40)$$

reveals a remarkably accurate approximate closed form for the error within the convergent region $|v| < V$:

$$I_M^{\{\tanh\}}(v) \simeq \frac{4e^{\frac{\pi\tau}{2}} (\pi \sin(\tau v) + 2v \cos(\tau v))}{(e^{\pi\tau} - 1)(4v^2 + \pi^2)} \quad (41)$$

From (41) we can deduce that within the convergent region the error will oscillate with approximate period of $\frac{2\pi}{\tau}$ and amplitude dependent on v and τ . Since τ increases with respect to M and $\lim_{\tau \rightarrow \infty} e^{\frac{\pi\tau}{2}} (e^{\pi\tau} - 1)^{-1} = 0$ we deduce from (40) and the exact expression (38) for $I_M^{\{\tanh\}}(v)$ that $\lim_{M \rightarrow \infty} I_M^{\{\tanh\}}(v) = 0$ as is required to achieve low error within $(-V, V)$.

E. An Improved ReLU Expansion

Here we expand $\operatorname{relu}(v)$, again following the method of Section III-A. Since the odd part, v , of $\operatorname{relu}(v)$ is trivial, we begin by expressing the even part in terms of its Fourier transform

$$|v| = -\frac{1}{\pi} \lim_{\rho \rightarrow \infty} \int_{-\rho}^{\rho} \frac{\cos(\xi v)}{\xi^2} d\xi. \quad (42)$$

We then apply our bound σ for integrals involving $\cos(v\xi)$ as per (29) so that we may expand the kernel as a partial sum and exchange the order of summation as per (12) yielding

$$|v| \simeq -\frac{1}{\pi} \sum_{m=0}^M \frac{(-1)^m v^{2m}}{(2m)!} \int_{-\sigma}^{\sigma} \xi^{2m-2} d\xi. \quad (43)$$

In this case, the integral is trivial. Solving directly and adding back in the odd part of $\operatorname{relu}(v)$ yields the desired formulas for the coefficients $R_{2m}(M)$ in Eq. (6).

$$\begin{aligned} \operatorname{relu}(v) &= \frac{v}{2} + \sum_{m=0}^M R_{2m}(M) v^{2m} + H_M^{\{\operatorname{relu}\}}(v) \\ &\simeq \frac{v}{2} + \sum_{m=0}^M R_{2m}(M) v^{2m} \quad \forall |v| < V, \end{aligned} \quad (44)$$

$$R_{2m}(M) = \frac{(-1)^{m+1} \sigma^{2m-1}}{\pi (2m)! (2m-1)!}. \quad (45)$$

Again, the precise remainder follows directly from application of (13):

$$H_M^{\{\text{relu}\}}(v) = -\frac{1}{\pi} \int_{\sigma}^{\infty} \frac{\cos(\xi v)}{\xi^2} d\xi \quad (46)$$

$$+ \frac{(-1)^M v^{2M+2}}{\pi(2M+2)!} \int_0^{\sigma} \xi^{2M} {}_1F_2(1; b_1, b_2; z) d\xi, \quad (47)$$

$$b_1 = M+2, b_2 = M+\frac{3}{2}, z = -\frac{v^2 \xi^2}{4}. \quad (48)$$

The integrals can be readily solved yielding

$$H_M^{\{\text{relu}\}}(v) = \frac{|v|}{2} - \frac{v \text{Si}(\sigma v)}{\pi} - \frac{\cos(\sigma v)}{\sigma} \quad (49)$$

$$+ \frac{(-1)^M \sigma^{2M+1} v^{2M+1}}{\pi(2M+2)(2M+1)!} {}_2F_3(1, a; b, b, c; z), \quad (50)$$

$$a = M + \frac{1}{2}, b = M + \frac{3}{2}, c = M + 2, z = -\frac{\sigma^2 v^2}{4}. \quad (51)$$

Due to the v^{2M+1} factor, the term of (50) dominates outside the region of convergence and is the source of expected divergence for $|v| \geq V$. Meanwhile, (49) dominates for small v leading to Gibbs-like oscillation within the region of convergence $|v| < V$. The exact expression for the oscillating component of the error, $I_M^{\{\text{relu}\}}(v)$, is given as

$$I_M^{\{\text{relu}\}}(v) = \frac{|v|}{2} - \frac{v \text{Si}(\sigma v)}{\pi} - \frac{\cos(\sigma v)}{\sigma}. \quad (52)$$

As with $\tanh(v)$, since σ increases with respect to the number of terms, M , and then since $\lim_{\sigma \rightarrow \infty} I_M^{\{\text{relu}\}}(v) = 0$ we can again deduce that $\lim_{M \rightarrow \infty} I_M^{\{\text{relu}\}}(v) = 0$ as is required to achieve low error within the convergent region.

F. Full Single Hidden Layer MLP Expansion

The coefficients, α_j , of the activations, φ , can then be used to expand the network under test as a multivariate polynomial. To perform this expansion, we substitute the hidden neuron input as defined in Eq. (4) into Eq. (2).

$$\varphi(v_n) \simeq \sum_{m=1}^M \alpha_j \left(b_n^{\{0\}} + \sum_{i=1}^{N_I} w_{n,i}^{\{0\}} x_i \right)^j, \quad j = 2m-1 \quad (53)$$

Applying multinomial expansion gives

$$\tanh(v_n) \simeq \sum_{m=1}^M \sum_{|\kappa|=j} \alpha_j \binom{j}{\kappa} v_n^{\kappa} x^{\kappa}, \quad (54)$$

$$v_n = \left(b_n^{\{0\}} \quad w_{n,1}^{\{0\}} \quad \dots \quad w_{n,N_I}^{\{0\}} \right). \quad (55)$$

Here $\kappa = [\kappa_1, \kappa_2, \dots, \kappa_{N_I+1}]$ is a multi-index where $u^{\kappa} = \prod_i u_i^{\kappa_i}$, $|\kappa| = \sum_i \kappa_i$, and $\binom{j}{\kappa} = \frac{j!}{\kappa_1! \kappa_2! \dots \kappa_{N_I+1}!}$ is a multinomial coefficient. The output of the network can then be approximated by taking the weighted sum of the neuron outputs:

$$y(\alpha, \beta, x) \simeq b^{\{1\}} + \sum_{n=1}^{N_H} \sum_{m=1}^M \sum_{|\kappa|=j} \alpha_j(M) \binom{j}{\kappa} w_n^{\{1\}} v_n^{\kappa} x^{\kappa} \quad (56)$$

We use $\Psi_{\kappa}(\alpha, \beta)$ to denote the coefficient associated with the term $x^{\kappa} = x_1^{\kappa_1} x_2^{\kappa_2} \dots x_{N_I+1}^{\kappa_{N_I+1}}$ in the polynomial approximation of $y(\beta, x)$. By definition of $\Psi_{\kappa}(\alpha, \beta)$ we can write:

$$y(\alpha, \beta, x) \simeq \sum_{\kappa} \Psi_{\kappa}(\alpha, \beta) x^{\kappa} \quad (57)$$

IV. EXPANSION RESULTS

To verify the analysis of Section III we evaluate the expansions for \tanh , relu , for various settings of the V parameter, which controls the maximum domain of validity, and number of terms M . In each evaluation, we first compare the approximate function values $\varphi_a(v) \simeq \sum_{m=0}^M \alpha_m v^m$ to the true function values $\varphi(v)$ over several values of v in $(-V-c, V+c)$ where c is small value chosen to show performance just outside of the domain of validity $(-V, V)$. We then show the measured error $E_M^{\{\varphi\}}(v) = \varphi(v) - \varphi_a(v)$, the exact error $H_M^{\{\varphi\}}(v)$, and the analytic approximate error $I_M^{\{\varphi\}}(v)$. Finally, we display the errors between the error formulas themselves and the measured errors, $|E_M^{\{\varphi\}}(v) - H_M^{\{\varphi\}}(v)|$ and $|E_M^{\{\varphi\}}(v) - I_M^{\{\varphi\}}(v)|$ for the exact error and analytic error approximation respectively.

The expansions and errors for \tanh are shown in Fig. 1 and 2, and for relu in Fig. 3 and 4. The formulas to compute the coefficients are evaluated in 450 digits of precision and the polynomials themselves are evaluated in IEEE 754 double precision floating point arithmetic. Satisfaction of the qualitative properties described in Table I is summarized in Table II. Qualitatively, we find that the *exact coeffs.*, *monic form*, *adjustable domain*, and *handles undef. derivs.* properties are satisfied by (30) and (44). The *explicit exact errors* property is satisfied by (32) and (33) for \tanh and by (49)-(51) for relu . Finally the *consistent method* property is satisfied by the steps of Section III-A.

V. CASE STUDY: APPLYING AMITE TO MLP EQUIVALENCE TESTING

A. Experimental Setup

The experimental process was modeled computationally on a Dell XPS Laptop. All computations were implemented in Python 3.7 using the pytorch, numpy, cupy, and mpmath libraries on an Nvidia GeForce GTX 1650 GPU with 1024 Cuda Cores and an Intel i9-9980HK CPU running at 2.40GHz. Parallel processing was implemented through standard pytorch and cupy matrix operations. Coefficients for \tanh and relu were precomputed using 450 digits of precision via the precise formulas of Section III and polynomials were evaluated at runtime in IEEE 754 double precision floating point arithmetic. General mathematical primitives including binomial and multinomial coefficients were precomputed and stored in hashmaps for fast access at runtime. Multinomial coefficient hashmaps required 4.73GB of disk space and were loaded into program memory as needed in chunks ranging from 11KB to 986MB for fast access.

B. Example Application

As an example application, we consider a single hidden layer MLP used in the control of a fielded hardware system. In such applications, it can be advantageous to rapidly develop models via open-source software tools [31]–[33] and then exploit the efficiency of numerous proposed hardware approaches for implementation [34]–[37]. However, separating design from implementation motivates the question: how do we confirm that the network implemented in hardware is

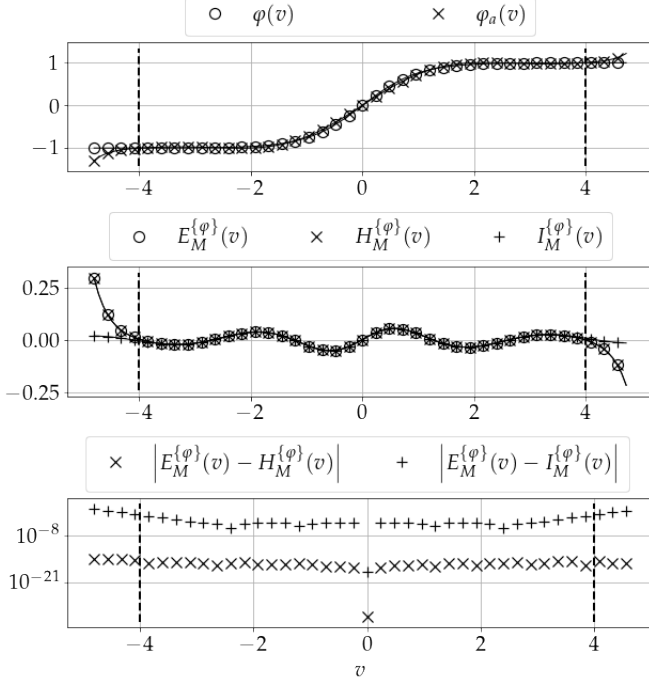
Hyperbolic Tangent Expansion for $M = 8, V = 4$ 

Fig. 1. Expansion results and errors for $\varphi(v) = \tanh(v)$, number of terms $M = 8$ and validity parameter $V = 4$. Top: expansion $\varphi_a(v)$ and true function $\varphi(v)$; middle: measured error $E_M^{\{\varphi\}}(v)$, exact error $H_M^{\{\varphi\}}(v)$, approximate error $I_M^{\{\varphi\}}(v)$; bottom: difference between measured errors and predicted errors.

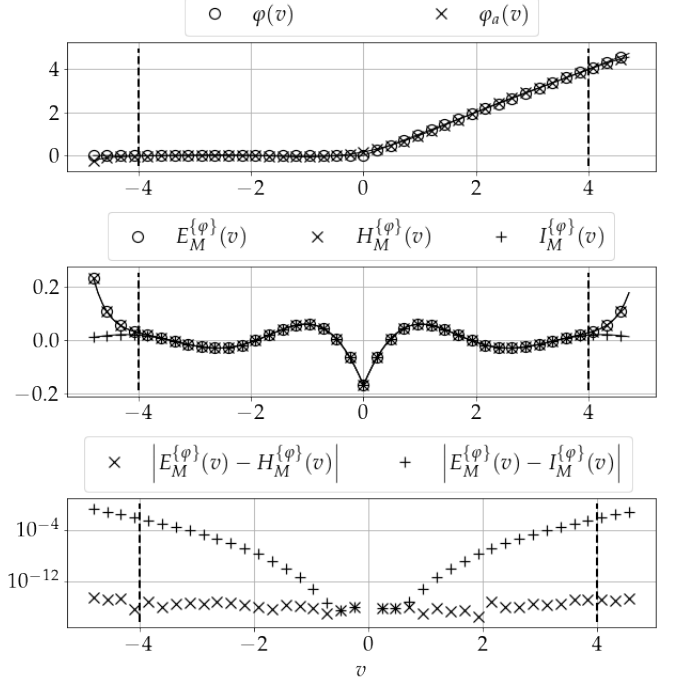
ReLU Expansion for $M = 8, V = 4$ 

Fig. 3. Expansion results and errors for $\varphi(v) = \text{relu}(v)$, number of terms $M = 8$ and validity parameter $V = 4$. Top: expansion $\varphi_a(v)$ and true function $\varphi(v)$; middle: measured error $E_M^{\{\varphi\}}(v)$, exact error $H_M^{\{\varphi\}}(v)$, approximate error $I_M^{\{\varphi\}}(v)$; bottom: difference between measured errors and predicted errors.

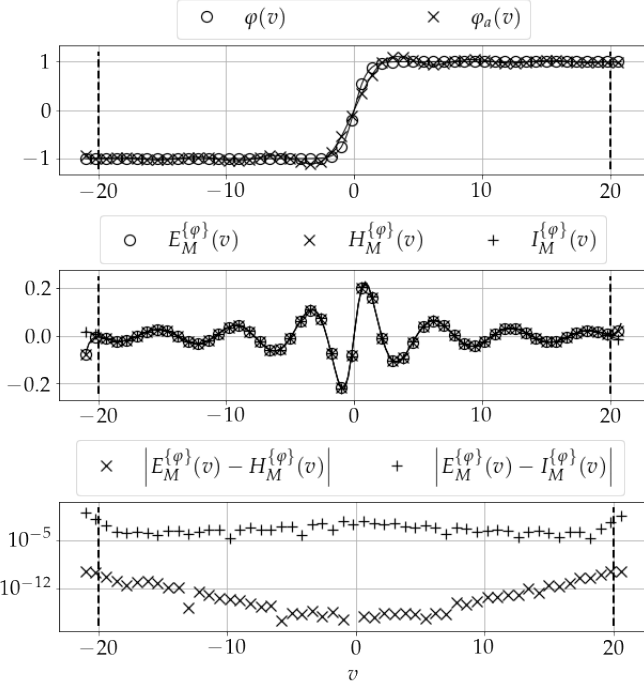
Hyperbolic Tangent Expansion for $M = 25, V = 20$ 

Fig. 2. Expansion results and errors for $\varphi(v) = \tanh(v)$, number of terms $M = 25$ and validity parameter $V = 20$. Top: expansion $\varphi_a(v)$ and true function $\varphi(v)$; middle: measured error $E_M^{\{\varphi\}}(v)$, exact error $H_M^{\{\varphi\}}(v)$, approximate error $I_M^{\{\varphi\}}(v)$; bottom: difference between measured errors and predicted errors.

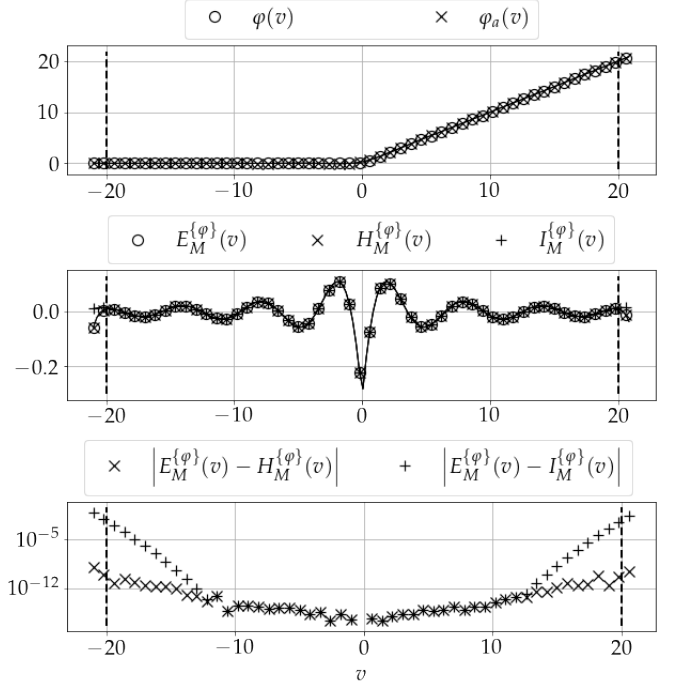
ReLU Expansion for $M = 25, V = 20$ 

Fig. 4. Expansion results and errors for $\varphi(v) = \text{relu}(v)$, number of terms $M = 25$ and validity parameter $V = 20$. Top: expansion $\varphi_a(v)$ and true function $\varphi(v)$; middle: measured error $E_M^{\{\varphi\}}(v)$, exact error $H_M^{\{\varphi\}}(v)$, approximate error $I_M^{\{\varphi\}}(v)$; bottom: difference between measured errors and predicted errors.

output-equivalent to the network originally designed? The answer is first complicated by equivalent symmetric configurations of a given network [38], [39] and by small perturbations in parameters yielding approximately equivalent input-output maps [40]. Due to nonlinearity, it is unclear what degree of output deviation represents a defect. Finally, measurement noise obscures the true error between the implemented input-output map and the original input-output map.

To show how AMITE can be applied here, we develop a bug-finding test to address the challenges above. First, we extract the weights of the implemented network following the methods of model stealing / replication [41]–[45] to fit a new model to a set of stimulus-response pairs. Then following the methods of Section III we convert the weights analytically to an AMITE polynomial representation and compare the coefficients to the AMITE representation of the original network. Here the AMITE coefficients provide a means to assess equivalence directly from the replicated and original weights. The preceding replication step is used to provide a guarantee that the stimulus applied yields suitable coverage to achieve a comprehensive equivalency test.

If the test signal does not provide sufficient coverage invalid weights will be extracted and the test will fail. This step biases the test towards a low false negative rate while offering the opportunity to further inspect a failed result by adding more test inputs. The observed efficacy of the equivalency test is dependent on the expansion technique’s ability to accurately and efficiently expand the entire MLP as a polynomial over a desired domain, and thus serves as empirical validation of the expansion technique’s utility, complementing the theoretical development in Section III.

C. MLP Equivalence Test Steps

The specific steps of the equivalency test used are as follows. First, an interrogation signal, $x_I(t)$, consisting of white noise fuzz vectors is activated to stimulate the implemented network. The measured output with any incurred measurement noise \mathcal{N} is collected and denoted $\hat{y}_I(t) = y(\alpha, \beta_I, x_I(t)) + \mathcal{N}$. The input and measurement output pairs (x_I, y_M) are then used to numerically solve for the replicated network weights β_R by fitting:

$$\beta_R = \arg \min_{\beta} \left((\hat{y}_I(t) - y(\alpha, \beta, x_I(t)))^2 \right) \quad (58)$$

Since the expected β values are known in advance, they are used as a starting point for fitting to expedite extraction of β_R and avoid false positives due to multiple local minima. The optimization problem is solved over 250 fuzz vectors x_I via stochastic gradient descent with adaptive learning rate starting at $l = 1 \times 10^{-3}$, weight decay $d = 0.01$, and no momentum. The original and replicated networks are then represented analytically via the methods of Section III-F as multivariate AMITE polynomials having coefficients $\Psi(\alpha, \beta_O) = [\Psi_{\kappa_n}(\alpha, \beta_O)]$ and $\Psi(\alpha, \beta_R) = [\Psi_{\kappa_n}(\alpha, \beta_R)]$

Example Bug Detection Test

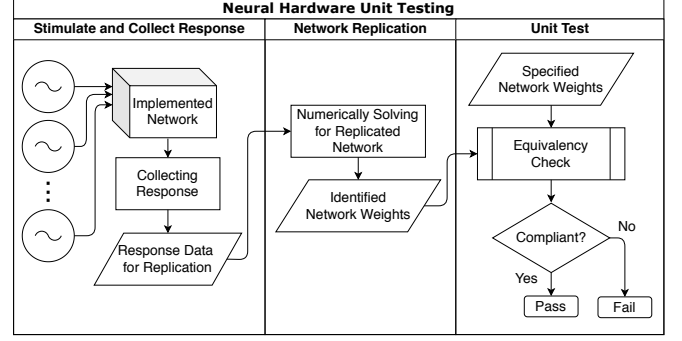


Fig. 5. Unit level bug-finding procedure applying network replication to test an implemented MLP for equivalence to an original MLP. An implemented network of known expected structure with unknown weights and unknown structure is stimulated by a plurality of signals and the unknown weights are identified from the response. The identified weights are converted to AMITE representations and checked for equivalency to the specified weights to determine if the networks match.

respectively. To check equivalency, we use a mean absolute logarithmic error between the magnitudes of the coefficients:

$$\eta(\Psi(\alpha, \beta_R), \Psi(\alpha, \beta_O)) = \text{mean} |\log(\epsilon + |\Psi(\alpha, \beta_O)|) - \log(\epsilon + |\Psi(\alpha, \beta_R)|)|. \quad (59)$$

If the error η is below a set threshold ϵ the networks are determined to be equivalent. These steps are summarized in Fig. 5.

D. Network Equivalency Testing Results

To collect results for the method of section V-C, a population of 90 MLPs is instantiated having inputs $N_I \in \{1, 2, 3\}$ and number of hidden nodes $N_H \in \{5, 10, 35, 75, 125\}$. The population is then duplicated to model a set of networks under test. Defects in the form of random weight perturbations are then introduced into half of the population of networks under test. The network equivalency test of Fig. 5 is executed following the methods of Section V-C on each network. All 90 networks are tested with different levels of noise $\mathcal{N} \in \{-20, -10, -1, 0, 1, 10, 20\}$. The entire procedure is repeated three times for a total of 1890 calls to the equivalency test. The accuracy of the equivalency test at finding bugs is reported in Fig. 6 with respect to signal to noise ratio in the measured outputs of the network under test. Runtime with respect to number of hidden nodes and number of inputs is reported in Fig. 7 and 8 respectively. For all tests an error threshold of $\epsilon = 0.01$ was applied when checking equivalency by the metric of (59): $\eta(\Psi(\alpha, \beta_R), \Psi(\alpha, \beta_O)) > \epsilon$. We find that the test completes in under 7 seconds on average for low-dimensional input (2-4 inputs) MLPs having up to 125 hidden nodes. The runtime per test is inclusive of both solving for the replicated network parameters and computing the AMITE polynomial representation.

VI. RELATED WORK

The work of this paper is intended to be of fundamental nature and applicable to several sub-fields of research in

Bug Detection Accuracy wrt. Measurement Noise

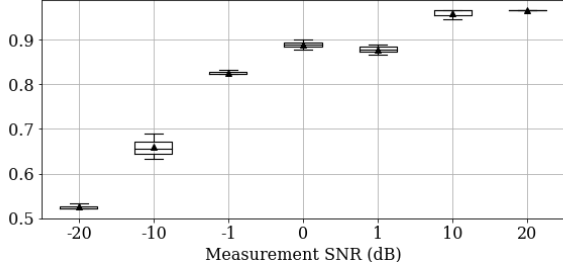


Fig. 6. Bug detection accuracy with respect to measurement noise. Shows the fraction of defective networks under test which were correctly identified. Results are aggregated over 1890 calls to the equivalency test on networks of varying sizes under various levels of noise.

neural networks, and is particularly related to neural systems verification, equivalency testing, to the study of sub-circuits within neural networks, and to model replication attacks. Recent relevant works in these domains are reviewed here.

Recent works on neural network verification focus on defense against and identification of adversarial perturbations [46], [47], output reachable set estimation [48], and computing upper bounds on error rates under adversarial attack [49]. Liu et al. survey algorithms for verifying deep neural networks and categorize them into forms of reachability analysis, optimization to falsify an assertion, and search to falsify an assertion [50]. Bunel et al. present a unifying framework for the formal verification of piecewise linear neural networks [51].

Other significant works present output range analysis via over-approximation [52] [53] and via exact (sound and complete) methods [54] [55], verification against a specification [56], and a hybrid systems approach to verifying properties of neural network controllers with sigmoid activations [57]. A survey of the safety and trustworthiness of deep neural networks is provided by Huang et al. [58]. A review of the state of the art in testing AI systems for safety and robustness is provided by Wu et al. [59].

Methods of identifying equivalent neural networks given a matrix of neuron outputs are available [60]–[63] and have recently been advanced by Kornblith et al. [64]. Methods to identify opportunities for compressing a neural network [65], [66] and for perturbing parameters to identify output-equivalent neural networks are also available [40]. We offer as a complement to these works a method of checking neural network equivalence (i.e. checking network under test compliance) by operating on the specified network weights and the replicated network weights without accessing the output signals of individual neurons. We also find that other network equivalency works and bug finding tests do not consider output noise present when measuring test vector responses.

It has recently been demonstrated that trained neural networks contain interpretable sub-circuits comprising semantic functions [67]–[71]. Building on feature visualization methods such as those from Erhan et al. [72], Simonyan et al. [73], and Mordvintsev et al. [74], a number of methods are now available to visualize individual sub-circuits inside neural networks [75]–[79]. Furthermore, stacking networks such as [80]–[83]

comprised of stacked smaller networks are good candidates for analysis via these techniques. We offer the methods of this paper as especially applicable to detailed study of such small sub-circuits within larger networks.

Runtime (s) wrt. Number of Hidden Units, (N_H)

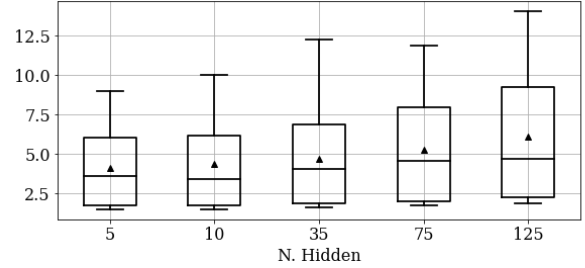


Fig. 7. Runtime per call to the test with respect to number of hidden units, N_H . Statistics are computed across 1890 calls to the test.

Runtime (s) wrt. Number of Inputs, (N_I)

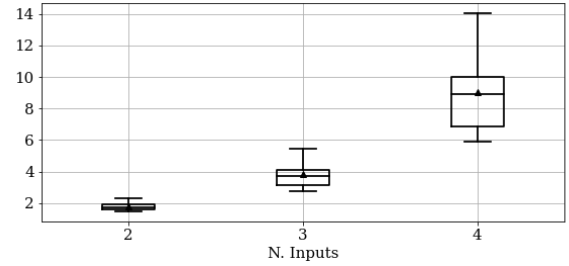


Fig. 8. Runtime per call to the test with respect to number of inputs, N_I . Statistics are computed across 1890 calls to the test.

VII. CONCLUSION

In this paper we have developed a novel polynomial expansion technique, the analytically modified integral transform expansion (AMITE), to enable for the first time decomposing neural network activation functions into polynomial forms having six advantageous properties, including exact formulas, monic form, adjustable domain, and robustness to undefined derivatives. To complement the exact formulas, convenient closed-form approximations of the exact expansion errors have been developed by exploiting relationships amongst the special functions arising therein. We have demonstrated that the exact error formulas match the measured expansion errors and shown the numerical error between the approximate error formulas and measured expansion errors. Using an MLP as a case study, we demonstrate the effectiveness of AMITE to the equivalency testing problem of MLP where a black-box network under test is stimulated, and a replicated multivariate polynomial form is efficiently extracted from a noisy response to enable comparison against an original network. We find that the test completes in under 7 seconds on average for low-dimensional input (2-4 inputs) MLPs having up to 125 hidden nodes. Our future work focuses on extending AMITE to neural networks with high-dimensional inputs.

APPENDIX A

Here we present a full derivation of the result of eq. (31) in section III. This equation gives the formula for the coefficients of the improved $\tanh(v)$ expansion and follows from the integral $\int \xi^j \operatorname{csch}(\frac{\pi}{2}\xi) d\xi$. We solve this integral by starting with a trivially more general one, $\int \xi^j \operatorname{sech}(a\xi + b) d\xi$, and exploiting the basic relation $\operatorname{sech}(a\xi + \frac{i\pi}{2}) = -i \operatorname{csch}(a\xi)$, between the hyperbolic functions such that the result may be readily applied to a class of related functions. Starting with repeated integration by parts

$$\begin{aligned} \int \xi^j \operatorname{sech}(a\xi + b) d\xi = \\ (-1)^j \int \frac{\partial^j}{\partial \xi^j} \xi^j \left(\underbrace{\int d\xi \cdots \int d\xi}_{j} \operatorname{sech}(a\xi + b) \right) d\xi \\ + \sum_{k=0}^{j-1} (-1)^k \frac{\partial^k}{\partial \xi^k} \xi^j \frac{\partial^{j-k-1}}{\partial \xi^{j-k-1}} \underbrace{\int d\xi \cdots \int d\xi}_{j} \operatorname{sech}(a\xi + b). \end{aligned} \quad (60)$$

Repeated differentiation of the hyperbolics is presented in full generality by [84]. Here we employ a simpler formula for repeated integration revealed by expressing $\operatorname{sech}(a\xi + b)$ in terms of the polylogarithms:

$$\begin{aligned} \underbrace{\int d\xi \cdots \int d\xi}_{j} \operatorname{sech}(a\xi + b) = \\ \frac{i(-1)^j}{a^j} (\operatorname{Li}_j(-ie^{-a\xi+b}) - \operatorname{Li}_j(ie^{-a\xi-b})). \end{aligned} \quad (61)$$

Applying to (60) yields the useful intermediate result

$$\int \xi^j \operatorname{sech}(a\xi + b) d\xi = -\frac{2}{a} \sum_{k=0}^j \frac{j! \xi^{j-k} \operatorname{Ti}_{k+1}(e^{-a\xi-b})}{a^k (j-k)!}. \quad (62)$$

Here $\operatorname{Ti}_s(z)$ denotes the Inverse Tangent Integral, defined by $\operatorname{Ti}_s(z) = \frac{1}{2i} (\operatorname{Li}_s(iz) - \operatorname{Li}_s(-iz))$. Noting the relationship $i\operatorname{Ti}_s(-iz) = \chi_s(z)$ and the relationship between $\operatorname{csch}(z)$ and $\operatorname{sech}(z)$ reveals

$$\begin{aligned} \Lambda_j(\xi) = \int \xi^j \operatorname{csch}(a\xi) d\xi \\ = -\frac{2}{a} \sum_{k=0}^j \frac{j! \xi^{j-k} \chi_{k+1}(e^{-a\xi})}{a^k (j-k)!}. \end{aligned} \quad (63)$$

The expression for the coefficient $T_{2m+1}(M)$ in (5) then follows directly from (15). The integral is evaluated to the bound τ corresponding to the kernel $\sin(\xi v)$ such that

$$T_{2m+1} = \frac{(-1)^m}{(2m+1)!} \int_0^\tau \xi^{2m+1} \operatorname{csch}\left(\frac{\pi}{2}\xi\right) d\xi \quad (64)$$

$$= \frac{(-1)^m}{(2m+1)!} \left(\Lambda_{2m+1}(\tau) - \lim_{\varepsilon \rightarrow 0} \Lambda_{2m+1}(\varepsilon) \right). \quad (65)$$

Noting that

$$\frac{1}{2} \lim_{\xi \rightarrow 0} \xi^{j-k} \operatorname{Li}_{k+1}\left(e^{-\frac{\pi\xi}{2}}\right) = \begin{cases} \frac{1}{2}\zeta(k+1) & j = k \\ 0 & j \neq k, \end{cases} \quad (66)$$

$$\begin{aligned} \frac{1}{2} \lim_{\xi \rightarrow 0} \xi^{j-k} \operatorname{Li}_{k+1}\left(-e^{-\frac{\pi\xi}{2}}\right) \\ = \begin{cases} \frac{1}{2}(2^{-k}-1)\zeta(k+1) & j = k \\ 0 & j \neq k, \end{cases} \end{aligned} \quad (67)$$

and the relation, $\zeta(2m) = (-1)^{m+1}(2\pi)^{2m} B_{2m} (2(2m)!)^{-1}$, between the Riemann Zeta function and the Bernoulli numbers yields the result of (31):

$$\begin{aligned} T_{2m+1}(M) = \frac{2^{2m+1}(4^{m+1}-1)B_{2m+2}}{(m+1)(2m+1)!} \\ + \frac{(-1)^{m+1}4}{\pi} \sum_{k=0}^{2m+1} \frac{2^k \tau^{2m+1-k} \chi_{k+1}(e^{-\frac{\pi\tau}{2}})}{\pi^k (2m+1-k)!}. \end{aligned}$$

REFERENCES

- [1] G. Montavon, S. Lapuschkin, A. Binder, W. Samek, and K.-R. Müller, "Explaining nonlinear classification decisions with deep Taylor decomposition," *Pattern Recognition*, vol. 65, pp. 211–222, May 2017. [Online]. Available: <https://linkinghub.elsevier.com/retrieve/pii/S0031320316303582>
- [2] S. Dutta, X. Chen, and S. Sankaranarayanan, "Reachability analysis for neural feedback systems using regressive polynomial rule inference," in *Proceedings of the 22nd ACM International Conference on Hybrid Systems: Computation and Control*. Montreal Quebec Canada: ACM, Apr. 2019, pp. 157–168. [Online]. Available: <https://dl.acm.org/doi/10.1145/3302504.3311807>
- [3] S. Obla, X. Gong, A. Aloufi, P. Hu, and D. Takabi, "Effective Activation Functions for Homomorphic Evaluation of Deep Neural Networks," *IEEE Access*, vol. 8, pp. 153 098–153 112, 2020. [Online]. Available: <https://ieeexplore.ieee.org/document/9169889/>
- [4] G. Lai, Z. Liu, Y. Zhang, and C. L. P. Chen, "Adaptive Position/Attitude Tracking Control of Aerial Robot With Unknown Inertial Matrix Based on a New Robust Neural Identifier," *IEEE Transactions on Neural Networks and Learning Systems*, vol. 27, no. 1, pp. 18–31, Jan. 2016. [Online]. Available: <http://ieeexplore.ieee.org/document/7061535/>
- [5] D. Nodland, H. Zargarzadeh, and S. Jagannathan, "Neural Network-Based Optimal Adaptive Output Feedback Control of a Helicopter UAV," *IEEE Transactions on Neural Networks and Learning Systems*, vol. 24, no. 7, pp. 1061–1073, Jul. 2013. [Online]. Available: <http://ieeexplore.ieee.org/document/6487408/>
- [6] B. Xu, D. Wang, Y. Zhang, and Z. Shi, "DOB-Based Neural Control of Flexible Hypersonic Flight Vehicle Considering Wind Effects," *IEEE Transactions on Industrial Electronics*, vol. 64, no. 11, pp. 8676–8685, Nov. 2017.
- [7] L. Shen, L. R. Margolies, J. H. Rothstein, E. Fluder, R. McBride, and W. Sieh, "Deep Learning to Improve Breast Cancer Detection on Screening Mammography," *Scientific Reports*, vol. 9, no. 1, p. 12495, Aug. 2019. [Online]. Available: <https://www.nature.com/articles/s41598-019-48995-4>
- [8] O.-A. Kwabena, Z. Qin, T. Zhuang, and Z. Qin, "MSCryptoNet: Multi-Scheme Privacy-Preserving Deep Learning in Cloud Computing," *IEEE Access*, vol. 7, pp. 29 344–29 354, 2019. [Online]. Available: <https://ieeexplore.ieee.org/document/8651459/>
- [9] "Hyperbolic tangent: Series representations (subsection 06/04)." [Online]. Available: <https://functions.wolfram.com/ElementaryFunctions/Tanh/06/04/>
- [10] C. Huang, J. Fan, W. Li, X. Chen, and Q. Zhu, "ReachNN: Reachability Analysis of Neural-Network Controlled Systems," *ACM Transactions on Embedded Computing Systems*, vol. 18, no. 5s, pp. 106:1–106:22, Oct. 2019. [Online]. Available: <https://doi.org/10.1145/3358228>
- [11] M. Vlček, "CHEBYSHEV POLYNOMIAL APPROXIMATION FOR ACTIVATION SIGMOID FUNCTION," *Neural Network World*, vol. 22, no. 4, pp. 387–393, 2012. [Online]. Available: <http://www.nnw.cz/obsahy12.html#22.023>

- [12] A. B. Koç and A. Kurnaz, "A new kind of double Chebyshev polynomial approximation on unbounded domains," *Boundary Value Problems*, vol. 2013, no. 1, p. 10, Dec. 2013. [Online]. Available: <https://boundaryvalueproblems.springeropen.com/articles/10.1186/1687-2770-2013-10>
- [13] B. K. Alpert and V. Rokhlin, "A Fast Algorithm for the Evaluation of Legendre Expansions," *SIAM Journal on Scientific and Statistical Computing*, vol. 12, no. 1, pp. 158–179, Jan. 1991. [Online]. Available: <https://epubs.siam.org/doi/abs/10.1137/0912009>
- [14] Y. Lee, J.-W. Lee, Y.-S. Kim, and J.-S. No, "Near-Optimal Polynomial for Modulus Reduction Using L2-Norm for Approximate Homomorphic Encryption," *IEEE Access*, vol. 8, pp. 144 321–144 330, 2020. [Online]. Available: <https://ieeexplore.ieee.org/document/9159551/>
- [15] D. Baptista and F. Morgado-Dias, "Low-resource hardware implementation of the hyperbolic tangent for artificial neural networks," *Neural Computing and Applications*, vol. 23, no. 3–4, pp. 601–607, Sep. 2013. [Online]. Available: <http://link.springer.com/10.1007/s00521-013-1407-x>
- [16] J.-W. Lee, E. Lee, Y. Lee, Y.-S. Kim, and J.-S. No, "High-precision bootstrapping of rms-ckks homomorphic encryption using optimal min-imax polynomial approximation and inverse sine function," *Cryptology ePrint Archive*, Report 2020/552, 2020, <https://eprint.iacr.org/2020/552>.
- [17] Y. Lee, J. Lee, Y.-S. Kim, H. Kang, and J.-S. No, "High-precision approximate homomorphic encryption by error variance minimization," *Cryptology ePrint Archive*, Report 2020/1549, 2020, <https://eprint.iacr.org/2020/1549>.
- [18] H. Bateman, A. Erdélyi, Bateman Manuscript Project, and USA, Eds., *Higher transcendental functions*, ser. California Institute of Technology Bateman Manuscript Project. New York, NY: McGraw-Hill, 1953.
- [19] A. P. Engelbrecht, "Using the Taylor expansion of multilayer feedforward neural networks," *South African Computer Journal*, vol. 2000, no. 26, pp. 181–189, Nov. 2000. [Online]. Available: <https://journals.co.za/content/comp/2000/26/EJC27886>
- [20] X. Chen, Q. Ma, and T. Alkharobi, "New neural networks based on taylor series and their research," in *2009 2nd IEEE International Conference on Computer Science and Information Technology*, Aug 2009, pp. 291–294.
- [21] D. Balduzzi, B. McWilliams, and T. Butler-Yeoman, "Neural Taylor approximations: convergence and exploration in rectifier networks," in *Proceedings of the 34th International Conference on Machine Learning - Volume 70*, ser. ICML'17. Sydney, NSW, Australia: JMLR.org, Aug. 2017, pp. 351–360.
- [22] D. Guo, Z. Nie, and L. Yan, "Novel Discrete-Time Zhang Neural Network for Time-Varying Matrix Inversion," *IEEE Transactions on Systems, Man, and Cybernetics: Systems*, vol. 47, no. 8, pp. 2301–2310, Aug. 2017.
- [23] A. S. Gaikwad and M. El-Sharkawy, "Pruning convolution neural network (squeezeNet) using taylor expansion-based criterion," in *2018 IEEE International Symposium on Signal Processing and Information Technology (ISSPIT)*, Dec. 2018, pp. 1–5, iSSN: 2162-7843.
- [24] I. S. Gradshteyn, I. M. Ryzhik, and A. Jeffrey, *Table of integrals, series, and products*, 7th ed. Amsterdam ; Boston: Academic Press, 2007.
- [25] M. AboulAtta, M. Ossadnik, and S.-A. Ahmadi, "Stabilizing Inputs to Approximated Nonlinear Functions for Inference with Homomorphic Encryption in Deep Neural Networks," *arXiv:1902.01870 [cs, stat]*, Feb. 2019, arXiv: 1902.01870. [Online]. Available: <http://arxiv.org/abs/1902.01870>
- [26] R. Bojanic and M. Vuilleumier, "On the rate of convergence of Fourier-Legendre series of functions of bounded variation," *Journal of Approximation Theory*, vol. 31, no. 1, pp. 67–79, Jan. 1981. [Online]. Available: <https://linkinghub.elsevier.com/retrieve/pii/S0021904581900319>
- [27] A. H. Namin, K. Leboeuf, R. Muscedere, H. Wu, and M. Ahmadi, "Efficient hardware implementation of the hyperbolic tangent sigmoid function," in *2009 IEEE International Symposium on Circuits and Systems*, May 2009, pp. 2117–2120, iSSN: 2158-1525.
- [28] A. Armato, L. Fanucci, E. Scilingo, and D. De Rossi, "Low-error digital hardware implementation of artificial neuron activation functions and their derivative," *Microprocessors and Microsystems*, vol. 35, no. 6, pp. 557–567, Aug. 2011. [Online]. Available: <https://linkinghub.elsevier.com/retrieve/pii/S0141933111000731>
- [29] G. Katz, D. A. Huang, D. Ibeling, K. Julian, C. Lazarus, R. Lim, P. Shah, S. Thakoor, H. Wu, A. Zeljić, D. L. Dill, M. J. Kochenderfer, and C. Barrett, "The Marabou Framework for Verification and Analysis of Deep Neural Networks," in *Computer Aided Verification*, ser. Lecture Notes in Computer Science, I. Dillig and S. Tasiran, Eds. Cham: Springer International Publishing, 2019, pp. 443–452.
- [30] H. Bateman, A. Erdelyi, W. Magnus, F. Oberhettinger, and F. G. Tricomi, *Integral Transforms*. New York: McGraw-Hill Book Company, 1954, vol. 1.
- [31] "scikit-learn: machine learning in Python — scikit-learn 0.22.2 documentation." [Online]. Available: <https://scikit-learn.org/stable/>
- [32] "PyTorch." [Online]. Available: <https://www.pytorch.org>
- [33] "TensorFlow." [Online]. Available: <https://www.tensorflow.org/>
- [34] J. Misra and I. Saha, "Artificial neural networks in hardware: A survey of two decades of progress," *Neurocomputing*, vol. 74, no. 1–3, pp. 239–255, Dec. 2010. [Online]. Available: <https://linkinghub.elsevier.com/retrieve/pii/S092523121000216X>
- [35] D. Maliuk and Y. Makris, "An Experimentation Platform for On-Chip Integration of Analog Neural Networks: A Pathway to Trusted and Robust Analog/RF ICs," *IEEE Transactions on Neural Networks and Learning Systems*, vol. 26, no. 8, pp. 1721–1734, Aug. 2015. [Online]. Available: <http://ieeexplore.ieee.org/lpdocs/epic03/wrapper.htm?arnumber=6901256>
- [36] A. M. Abdelsalam, J. M. P. Langlois, and F. Cheriet, "Accurate and Efficient Hyperbolic Tangent Activation Function on FPGA using the DCT Interpolation Filter," *arXiv:1609.07750 [cs]*, Sep. 2016, arXiv: 1609.07750. [Online]. Available: <http://arxiv.org/abs/1609.07750>
- [37] C. D. Schuman, T. E. Potok, R. M. Patton, J. D. Birdwell, M. E. Dean, G. S. Rose, and J. S. Plank, "A Survey of Neuromorphic Computing and Neural Networks in Hardware," *arXiv:1705.06963 [cs]*, May 2017, arXiv: 1705.06963. [Online]. Available: <http://arxiv.org/abs/1705.06963>
- [38] H. J. Sussmann, "Uniqueness of the weights for minimal feedforward nets with a given input-output map," *Neural Networks*, vol. 5, no. 4, pp. 589–593, Jul. 1992. [Online]. Available: <https://linkinghub.elsevier.com/retrieve/pii/S0893608005800371>
- [39] F. Albertini and E. D. Sontag, "Uniqueness of Weights for Neural Networks," in *Artificial Neural Networks for Speech and Vision*. Chapman and Hall, London, 1993, pp. 113–125.
- [40] C. DiMattina and K. Zhang, "How to Modify a Neural Network Gradually Without Changing Its Input-Output Functionality," *Neural Computation*, vol. 22, no. 1, pp. 1–47, Jan. 2010. [Online]. Available: <http://www.mitpressjournals.org/doi/10.1162/neco.2009.05-08-781>
- [41] F. Tramèr, F. Zhang, A. Juels, M. K. Reiter, and T. Ristenpart, "Stealing machine learning models via prediction apis," in *Proceedings of the 25th USENIX Conference on Security Symposium*, ser. SEC'16. USA: USENIX Association, 2016, p. 601–618.
- [42] N. Papernot, P. McDaniel, I. Goodfellow, S. Jha, Z. B. Celik, and A. Swami, "Practical Black-Box Attacks against Machine Learning," in *Proceedings of the 2017 ACM on Asia Conference on Computer and Communications Security - ASIA CCS '17*. Abu Dhabi, United Arab Emirates: ACM Press, 2017, pp. 506–519. [Online]. Available: <http://dl.acm.org/citation.cfm?doid=3052973.3053009>
- [43] S. J. Oh, B. Schiele, and M. Fritz, *Towards Reverse-Engineering Black-Box Neural Networks*. Cham: Springer International Publishing, 2019, pp. 121–144. [Online]. Available: https://doi.org/10.1007/978-3-030-28954-6_7
- [44] V. Duddu, D. Samanta, D. V. Rao, and V. E. Balas, "Stealing neural networks via timing side channels," *ArXiv*, vol. abs/1812.11720, 2018.
- [45] T. Orekondy, B. Schiele, and M. Fritz, "Knockoff Nets: Stealing Functionality of Black-Box Models," in *2019 IEEE/CVF Conference on Computer Vision and Pattern Recognition (CVPR)*. Long Beach, CA, USA: IEEE, Jun. 2019, pp. 4949–4958. [Online]. Available: <https://ieeexplore.ieee.org/document/8953839/>
- [46] B. Darvish Rouani, M. Samragh, T. Javidi, and F. Koushanfar, "Safe Machine Learning and Defeating Adversarial Attacks," *IEEE Security & Privacy*, vol. 17, no. 2, pp. 31–38, Mar. 2019. [Online]. Available: <https://ieeexplore.ieee.org/document/8677311/>
- [47] A. Venzke and S. Chatzivasileiadis, "Verification of Neural Network Behaviour: Formal Guarantees for Power System Applications," *arXiv:1910.01624 [cs, eess, math]*, Jan. 2020, arXiv: 1910.01624. [Online]. Available: <http://arxiv.org/abs/1910.01624>
- [48] W. Xiang, H.-D. Tran, and T. T. Johnson, "Output Reachable Set Estimation and Verification for Multilayer Neural Networks," *IEEE Transactions on Neural Networks and Learning Systems*, vol. 29, no. 11, pp. 5777–5783, Nov. 2018. [Online]. Available: <https://ieeexplore.ieee.org/document/8318388/>
- [49] K. Dvijotham, R. Stanforth, S. Gowal, C. Qin, S. De, and P. Kohli, "Efficient neural network verification with exactness characterization," in *UAI*, 2019.
- [50] C. Liu, T. Arnon, C. Lazarus, C. W. Barrett, and M. J. Kochenderfer, "Algorithms for verifying deep neural networks," *ArXiv*, vol. abs/1903.06758, 2019.

- [51] R. R. Bunel, I. Turkaslan, P. Torr, P. Kohli, and P. K. Mudigonda, "A unified view of piecewise linear neural network verification," in *Advances in Neural Information Processing Systems 31*, S. Bengio, H. Wallach, H. Larochelle, K. Grauman, N. Cesa-Bianchi, and R. Garnett, Eds. Curran Associates, Inc., 2018, pp. 4790–4799. [Online]. Available: <http://papers.nips.cc/paper/7728-a-unified-view-of-piecewise-linear-neural-network-verification.pdf>
- [52] T. Gehr, M. Mirman, D. Drachler-Cohen, P. Tsankov, S. Chaudhuri, and M. Vechev, "AI2: Safety and Robustness Certification of Neural Networks with Abstract Interpretation," in *2018 IEEE Symposium on Security and Privacy (SP)*, May 2018, pp. 3–18, iSSN: 2375-1207.
- [53] C. Huang, J. Fan, X. Chen, W. Li, and Q. Zhu, "Divide and Slide: Layer-Wise Refinement for Output Range Analysis of Deep Neural Networks," *IEEE Transactions on Computer-Aided Design of Integrated Circuits and Systems*, vol. 39, no. 11, pp. 3323–3335, Nov. 2020.
- [54] H. D. Tran, X. Yang, D. M. Lopez, P. Musau, L. V. Nguyen, W. Xiang, S. Bak, and T. T. Johnson, "NNV: The Neural Network Verification Tool for Deep Neural Networks and Learning-Enabled Cyber-Physical Systems," in *Computer Aided Verification - 32nd International Conference, CAV 2020, Proceedings*. Springer, 2020, pp. 3–17. [Online]. Available: <https://augusta.pure.elsevier.com/en/publications/nnv-the-neural-network-verification-tool-for-deep-neural-networks>
- [55] H.-D. Tran, P. Musau, D. Manzanar Lopez, X. Yang, L. V. Nguyen, W. Xiang, and T. T. Johnson, "Parallelizable Reachability Analysis Algorithms for Feed-Forward Neural Networks," in *2019 IEEE/ACM 7th International Conference on Formal Methods in Software Engineering (FormalSE)*. Montreal, QC, Canada: IEEE, May 2019, pp. 51–60. [Online]. Available: <https://ieeexplore.ieee.org/document/8807491/>
- [56] S. YAGHOUBI and G. FAINEKOS, "Worst-case Satisfaction of STL Specifications Using Feedforward Neural Network Controllers: A Lagrange Multipliers Approach," in *2020 Information Theory and Applications Workshop (ITA)*, Feb. 2020, pp. 1–20, iSSN: 2642-7338.
- [57] R. Ivanov, J. Weimer, R. Alur, G. J. Pappas, and I. Lee, "Verisig: verifying safety properties of hybrid systems with neural network controllers," in *Proceedings of the 22nd ACM International Conference on Hybrid Systems: Computation and Control*, ser. HSCC '19. Montreal, Quebec, Canada: Association for Computing Machinery, Apr. 2019, pp. 169–178. [Online]. Available: <https://doi.org/10.1145/3302504.3311806>
- [58] X. Huang, D. Kroening, W. Ruan, J. Sharp, Y. Sun, E. Thamo, M. Wu, and X. Yi, "A survey of safety and trustworthiness of deep neural networks: Verification, testing, adversarial attack and defence, and interpretability," *Computer Science Review*, vol. 37, p. 100270, Aug. 2020. [Online]. Available: <https://linkinghub.elsevier.com/retrieve/pii/S1574013719302527>
- [59] T. Wu, Y. Dong, Z. Dong, A. Singa, X. Chen, and Y. Zhang, "Testing Artificial Intelligence System Towards Safety and Robustness: State of the Art," *IAENG International Journal of Computer Science*, vol. 47, no. 3, Sep. 2020.
- [60] A. Laakso and G. Cottrell, "Content and cluster analysis: Assessing representational similarity in neural systems," *Philosophical Psychology*, vol. 13, no. 1, pp. 47–76, Mar. 2000. [Online]. Available: <http://www.tandfonline.com/doi/abs/10.1080/09515080050002726>
- [61] Y. Li, J. Yosinski, J. Clune, H. Lipson, and J. Hopcroft, "Convergent Learning: Do different neural networks learn the same representations?" in *Journal of Machine Learning Research Conference Proceedings*, 2015, pp. 196–212.
- [62] M. Raghu, J. Gilmer, J. Yosinski, and J. Sohl-Dickstein, "Svcca: Singular vector canonical correlation analysis for deep learning dynamics and interpretability," in *Advances in Neural Information Processing Systems 30*, I. Guyon, U. V. Luxburg, S. Bengio, H. Wallach, R. Fergus, S. Vishwanathan, and R. Garnett, Eds. Curran Associates, Inc., 2017, pp. 6076–6085. [Online]. Available: <http://papers.nips.cc/paper/7188-svcca-singular-vector-canonical-correlation-analysis-for-deep-learning-dynamics-and-interpretability.pdf>
- [63] A. Morcos, M. Raghu, and S. Bengio, "Insights on representational similarity in neural networks with canonical correlation," in *Advances in Neural Information Processing Systems 31*, S. Bengio, H. Wallach, H. Larochelle, K. Grauman, N. Cesa-Bianchi, and R. Garnett, Eds. Curran Associates, Inc., 2018, pp. 5727–5736. [Online]. Available: <http://papers.nips.cc/paper/7815-insights-on-representational-similarity-in-neural-networks-with-canonical-correlation.pdf>
- [64] S. Kornblith, M. Norouzi, H. Lee, and G. Hinton, "Similarity of Neural Network Representations Revisited," in *Proceedings of the 36th International Conference on Machine Learning*, Long Beach, CA, USA, 2019.
- [65] C.-H. Chang, "Deep and Shallow Architecture of Multilayer Neural Networks," *IEEE Transactions on Neural Networks and Learning Systems*, vol. 26, no. 10, pp. 2477–2486, Oct. 2015. [Online]. Available: <http://ieeexplore.ieee.org/document/7010967/>
- [66] H. Huang and H. Yu, "LTNN: A Layerwise Tensorized Compression of Multilayer Neural Network," *IEEE Transactions on Neural Networks and Learning Systems*, vol. 30, no. 5, pp. 1497–1511, May 2019. [Online]. Available: <https://ieeexplore.ieee.org/document/8480873/>
- [67] A. Karpathy, J. Johnson, and L. Fei-Fei, "Visualizing and Understanding Recurrent Networks," *arXiv:1506.02078 [cs]*, Nov. 2015, arXiv: 1506.02078. [Online]. Available: <http://arxiv.org/abs/1506.02078>
- [68] B. Zhou, A. Khosla, A. Lapedriza, A. Oliva, and A. Torralba, "Object Detectors Emerge in Deep Scene CNNs," *arXiv:1412.6856 [cs]*, Apr. 2015, arXiv: 1412.6856. [Online]. Available: <http://arxiv.org/abs/1412.6856>
- [69] D. Bau, B. Zhou, A. Khosla, A. Oliva, and A. Torralba, "Network Dissection: Quantifying Interpretability of Deep Visual Representations," *arXiv:1704.05796 [cs]*, Apr. 2017, arXiv: 1704.05796. [Online]. Available: <http://arxiv.org/abs/1704.05796>
- [70] A. Gonzalez-Garcia, D. Modolo, and V. Ferrari, "Do semantic parts emerge in Convolutional Neural Networks?" *arXiv:1607.03738 [cs]*, Sep. 2017, arXiv: 1607.03738. [Online]. Available: <http://arxiv.org/abs/1607.03738>
- [71] C. Olah, N. Cammarata, L. Schubert, G. Goh, M. Petrov, and S. Carter, "Zoom in: An introduction to circuits," *Distill*, 2020, <https://distill.pub/2020/circuits/zoom-in>.
- [72] D. Erhan, Y. Bengio, A. Courville, and P. Vincent, "Visualizing higher-layer features of a deep network," *Technical Report, Université de Montréal*, 01 2009.
- [73] K. Simonyan, A. Vedaldi, and A. Zisserman, "Deep Inside Convolutional Networks: Visualising Image Classification Models and Saliency Maps," *arXiv:1312.6034 [cs]*, Apr. 2014, arXiv: 1312.6034. [Online]. Available: <http://arxiv.org/abs/1312.6034>
- [74] A. Mordvintsev and M. Olah, Christopher Tyka, "Inceptionism: Going Deeper into Neural Networks," 2015. [Online]. Available: <http://ai.googleblog.com/2015/06/inceptionism-going-deeper-into-neural.html>
- [75] A. Nguyen, A. Dosovitskiy, J. Yosinski, T. Brox, and J. Clune, "Synthesizing the preferred inputs for neurons in neural networks via deep generator networks," *arXiv:1605.09304 [cs]*, Nov. 2016, arXiv: 1605.09304. [Online]. Available: <http://arxiv.org/abs/1605.09304>
- [76] A. Nguyen, J. Clune, Y. Bengio, A. Dosovitskiy, and J. Yosinski, "Plug & Play Generative Networks: Conditional Iterative Generation of Images in Latent Space," *arXiv:1612.00005 [cs]*, Apr. 2017, arXiv: 1612.00005. [Online]. Available: <http://arxiv.org/abs/1612.00005>
- [77] C. Olah, A. Mordvintsev, and L. Schubert, "Feature visualization," *Distill*, 2017, <https://distill.pub/2017/feature-visualization>.
- [78] F. Hohman, H. Park, C. Robinson, and D. H. Chau, "Summit: Scaling Deep Learning Interpretability by Visualizing Activation and Attribution Summarizations," *arXiv:1904.02323 [cs]*, Sep. 2019, arXiv: 1904.02323. [Online]. Available: <http://arxiv.org/abs/1904.02323>
- [79] S. Carter, Z. Armstrong, L. Schubert, I. Johnson, and C. Olah, "Activation atlas," *Distill*, 2019, <https://distill.pub/2019/activation-atlas>.
- [80] L. Deng, D. Yu, and J. Platt, "Scalable stacking and learning for building deep architectures," in *2012 IEEE International Conference on Acoustics, Speech and Signal Processing (ICASSP)*, Mar. 2012, pp. 2133–2136, iSSN: 2379-190X.
- [81] L. Deng, X. He, and J. Gao, "Deep stacking networks for information retrieval," in *2013 IEEE International Conference on Acoustics, Speech and Signal Processing*, May 2013, pp. 3153–3157, iSSN: 2379-190X.
- [82] J. Wang, K. Feng, and J. Wu, "SVM-Based Deep Stacking Networks," *Proceedings of the AAAI Conference on Artificial Intelligence*, vol. 33, pp. 5273–5280, Jul. 2019. [Online]. Available: <http://www.aaai.org/ojs/index.php/AAAI/article/view/4463>
- [83] A. Khamparia, D. Gupta, N. G. Nguyen, A. Khanna, B. Pandey, and P. Tiwari, "Sound Classification Using Convolutional Neural Network and Tensor Deep Stacking Network," *IEEE Access*, vol. 7, pp. 7717–7727, 2019. [Online]. Available: <https://ieeexplore.ieee.org/document/8605515/>
- [84] M. I. Qureshi, S. Porwal, D. Ahamad, and K. A. Quraishi, "Successive differentiations of tangent, cotangent, secant, cosecant functions and related hyperbolic functions (A hypergeometric approach)," *International Journal of Mathematics Trends and Technology*, vol. 65, no. 7, pp. 325–367, Jul. 2019. [Online]. Available: <http://www.ijmtjournal.org/archive/ijmtt-v65i7p541>